MedCrave
Step into the World of Research
International Journal of Complementary & Alternative Medicine

Research Article

Open Access
CrossMark

Monte Carlo calculation of absorbed dose in breast radiotherapy due to photon beams of different energies

Abstract

In this study, breast cancer treatment reproduced from a VARIAN eclipse planning system is simulated. This treatment was simulate using the Monte Carlo system. To this end, the body of the woman is simulate by the geometry of the Phantom FAX06, which was reproduced using the ImageJ software that allowed the import and conversion of DICOM images into valid input files for the MCNPX code. Additionally, geometry of the linear accelerator head (including the MLC) was constructed. Co-60 photons, 6 and 15 MV photon spectra were simulate with an angle that allowed for the recreation of two tangential fields used in conventional radiation therapy treatments for breast cancer. The main objective of this study was to estimate the absorbed dose in each of the organs involved in this type of treatment and for each of the sources simulated. The result allowed us to establish the differences between the absorbed dose that is transferred to the target organ and that which is transferred to the organs at risk, such as the heart and lungs. The dose absorbed in organs at risk and target organ when Co-60 is used has advantages over the use of 6 and 15 MV beams, these results should be considered by the manufacturers of LINAC'S and by the scientific community. The proposal in this sense is to manufacture a device with Co-60 and with the technology of a LINAC for the treatment of some cancer.

Keywords: monte carlo, MCNPX code, radiotherapy, breast cancer, absorbed dose

Volume 15 Issue 3 - 2022

S.A. Martinez-Ovalle,[1,2] M. Díaz-Lagos,[1] J.A. Diaz-Merchan,[1,2] J. S. Estepa-Jiménez[1,2]

[1]Universidad Pedagógica y Tecnológica de Colombia, Tunja, Colombia

[2]Centro de Cancerología de Boyacá, Tunja, Colombia

Correspondence: J. S. Estepa-Jiménez, Universidad Pedagógica y Tecnológica de Colombia, Avenida Central del Norte 39-115 (Applied Nuclear Physics and Simulation Group), Tel (+57) 3208513790, Tunja, Colombia, Email: juansebastian.estepa@uptc.edu.co

Received: May 28, 2022 | **Published:** June 23, 2022

Abbreviations: LINAC, linear accelerator; MLC, multileaf collimator; MV, mega voltage; IMRT, intensity-modulated radiation therapy; VMAT, volumetric modulated arc therapy; MeV, Megaelectronvolt; SSD, Source to surface distance

Introduction

Around 5% of illnesses in the world are related to malignant tumors in both men and women. In Latin America and the Caribbean, for example, approximately 100,000 cases have been reported per year, and breast cancer is one of the most common among women worldwide. This type of malignancy is worthy of any type of research that involves not only prevention, but also the implementation of treatments and techniques focused on reducing deaths and improving the quality of life in patients.[1]

In recent decades, the prevention, discovery, and treatment of breast cancer have transformed in a way that over 90% of cases have been diagnosed in the early stages, and more effective treatments have been implemented with the different types of radiation therapy (conventional, IMRT, VMAT, etc.). After years of studies, it has been shown that said treatments reduce the recurrence of the local rate by approximately 70% after a mastectomy or after a more conservative method of breast cancer treatment, and that in reality they could increase the survival rate of higher-risk patients after treatment with radical surgeries and systematic adjuvant therapies.[2]

External radiotherapy in breast cancer can be provided through the use of equipment that uses encapsulated sources of radioactive materials such as the Co-60.[3,4] This isotope mainly emits gamma-ray photons with an energy of 1.17 and 1.33 MeV, and nowadays devices of last generation as Gamma Knife show excellent results in localized brain tumors.[5] Nevertheless, the last generation of LINAC's operates at different energies; however, the dual energies of 6 and 15 MV or 6 and 18 MV are the most used. This equipment shows a very good absorbed-dose distribution in the area of treatment, and also the reduction of the dose absorbed by the healthy surrounding tissue.[6] Because of this, treatments have shifted away from the conventional radiation therapies with Co-60,[7] which are evaluated in this study.

The Monte Carlo Method has been used in various types of research, for example, to extract the properties of absorption, dispersion, and malignant and non-malignant tissue fluorescence, and to diagnose breast cancer according to these intrinsic properties of the tissue.[8,9]

Modulated electron radiation therapy (MERT), intensity-modulated radiotherapy (IMRT), and conventional tangential photon beams have been evaluated in the treatment of breast cancer to perform optimizations in treatment with various energy beams, always seeking a reduction of the maximum dose to the lungs.[10] Monte Carlo method has been used to estimate the dose distribution in mammography using, a source term, the photon spectrum produced by a tube of X-rays.[11] Monte Carlo (MC) calculations is the only way to obtain detailed information about photon and electron spectra produced by devices emitting ionizing radiation.[12] The different codes used for this purpose turn out to be a fundamental tool for research in this field.[13-17] All these studies agree on the importance of studying the most appropriate photon energies that should be used in the treatment of each malignant disease, here is the importance of this study.

The objective of this work is to compare the differences in the absorbed dose that is supplied to organs and tissues when three photon beams are used during a conventional treatment of breast cancer. The result allows to demonstrate the advantages of using a low-energy beam like that of Co-60 abandoned by manufacturing houses today.

Material and methods

A FAX06 phantom was used,[18] which was reproduced with ImageJ,[19] which allows for the reproduction of the female body for the MCNPX code.[20]

Images of the treatment field were taken in the planning of conventional radiation therapy using the Varian Eclipse planning system.[21] The simulated patient was treated with a VARIAN C/D Linear Accelerator operating at 6 and 15 MV. The accelerator head is simulated by the geometry shown in figure 1.[22] Figure 1 shows the two tangential fields that were reproduced.

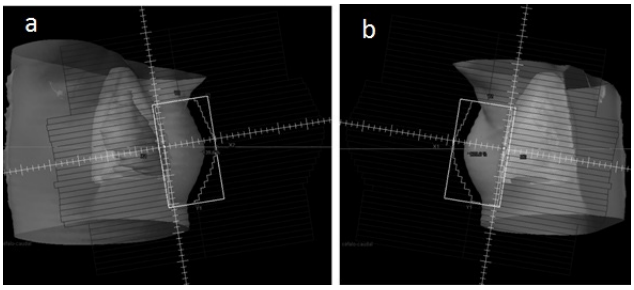

Figure 1 Breast planning treatment, taken using the Varian Eclipse planning system. a) Internal Tangential Field. b) External Tangential Field.

The planning system shown in Figure 1 corresponds to a 3D radiation therapy treatment with two tangential treatment fields.

The geometry of the female torso and all of its organs were reconstructed using ImageJ. A total of 9057.68 voxels of 3·3·3 mm^3 (with differing densities and composition according to the organ to which they pertain) reproduced the phantom (Figure 2). The elemental composition of each organ and tissue was taken from.[23]

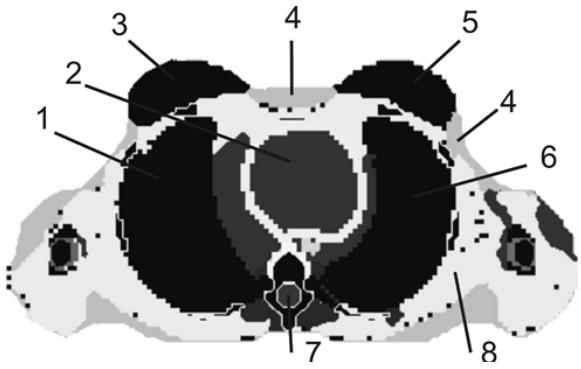

Figure 2 Cross section of the phantom FAX06. Left breast (5), right breast (3), heart (2), right lung (1), left lung (6), skin (4), marrow (7), and muscle (8).

The simplified geometry of the head of the LINAC consists of a spherical shielding made up of high-density materials (Pb and W), with radius of 26.75cm and 8.331cm respectively. Two independent simulations for each energy beam is launched from the head of the LINAC. Table 1 shows the elementary composition of the materials used in the simulation.

Table 1 Characteristics of materials

Material	Density (g/cm³)	Composition
Breast	1.04	H (11.6%) + C (51.9%) + N (36.5%)
Air	0.001225	O (22%) + C (2.5%) + N (75%) + Ar (0.5%)
W	19.3	W (100%)
Pb	11.4	Pb (100%)
Heart	1.05	H (10.4%) + C (13.9%) + N (2.9%) + O (71.85%) + Na (0.1%) + P (0.2%) + S (0.2%) + Cl (0.3%) + K (0.3%)
Lung	1.049	H (10.3%) + C (10.5%) + N (3.1%) + O (74.9%) + Na (0.2%) + P (0.2%) + S (0.3%) + Cl (0.3%) + K (0.2%)
Marrow	0.97	H (11.5%) + C (64.4%) + N (0.7%) + O (23.1%) + Na (0.1%) + S (0.1%) + Cl (0.1%)
Muscle	1.04	H (10.2%) + C (14.3%) + N (3.4%) + O (71%) + Na (0.1%) + P (0.2%) + S (0.3%) + Cl (0.1%) + K (0.4%)

The two tangential fields were recreated for adjustment to the planning shown in Figure 1, for which the multi-leaf collimator (MLC) system was constructed as well (Figure 3). Figure 4 shows the full geometry used in the simulation with the location of the LINAC head in the two orientations, for the external tangential field and for the internal tangential field.

A total of six simulations, positioning the MLC system at 30cm SSD for ^{60}Co and at 50cm SSD for the simulation of the spectra of 6 and 15 MV. Each of the spectra is launched from the geometric center of the first sphere of W that simulates the head of the LINAC, emitting isotropically. These calculations were achieved in the parallelized cluster, simulating a total of $6.4 \cdot 10^8$ stories for ^{60}Co, 9.6 □ 10^8 histories for 6 MV and $7.2 \cdot 10^8$ stories for 15 MV. The energy cutoff for photons and electrons was established in 0.001 MeV, for the head shield 0.521 MeV.

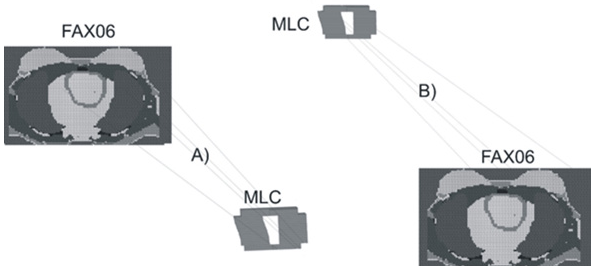

Figure 3 Phantom and MLC geometries used in the simulation. A) External Tangential Field B) Internal Tangential Field.

Figure 5 shows the three spectra used in the simulation, plot in black corresponds to Co-60, plot in Red corresponds to 15 MV spectra and plot in blue corresponds to 6 MV spectra.

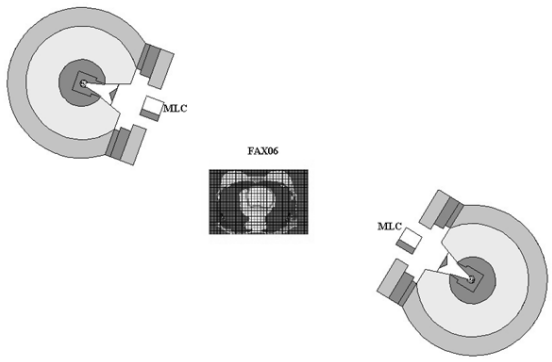

Figure 4 Full geometry of the simulation (XZ plane).

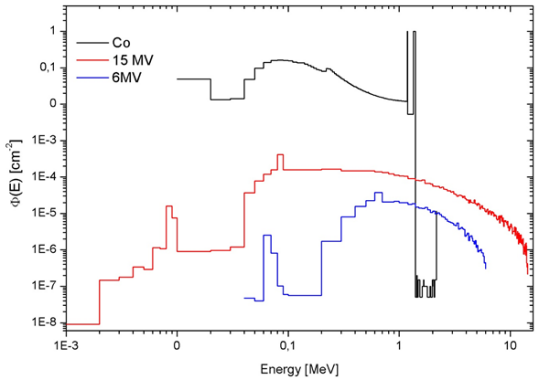

Figure 5 Spectral photon fluence used in the calculations. Red spectrum is taken from,[23] Blue (this study) and black (this study).

Results and discussion

The objective of each simulation was to study the absorbed dose in each of the organs and tissues when used with the three types of beams. Figure 6 shows the calculations of the absorbed dose independently for each of the orientations shown in Figure 3. The absorbed dose is calculated from the tally * f8 that gives deposited energy, this value is divided by the mass of each one of the organs and tissues.

In Figure 6, the same pattern of behavior in the transfer of energy is observed for both orientations A and B, with more energy resulting in a higher dose. The majority of the contributions went to the left breast as expected, Organ (10), followed by muscle (4) adipose tissue (6), skin (1), and the left lung (8), both in the internal tangential field and the external tangential field. In Table 2 is shown the absorbed dose per history for both photon beam orientations. The internal tangential field contributed a higher absorbed dose in the breast and skin, while the bone received a higher dose in the external field. This result allows to establish that the higher the energy, the higher the dose absorbed in the organs and tissues, however, this does not imply that the highest energy is the ideal in the treatment, because it should not be forgotten that there is a spectrum in each case and experience shows that in some treatments, beam combinations of 6 and 15 MV give good results depending on the size of the breast.

For the lung, the greatest contribution is due to the external tangential field when using 6 MV and Co-60 beams. With a beam of 15 MV, the greatest contribution in lung is due to the internal tangential field. The heart received the largest contribution from the three beams was in the external tangential field. The relative error associated with the calculation in all the cases was < 0.01.

In comparing the fields, it is evident that the majority of the contributions of the absorbed dose in the breast are related to the internal tangential field. The radiation beam of 15MV transfers the greatest quantity of absorbed dose to all of the organs and tissues in the two orientations, due to a large spectrum of photons of up to 15 MeV that pass through the patient. Regarding the heart, we noticed that the absorbed dose that this organ receives is lower in the internal tangential field. The contribution of the two fields is presented in Table 3. It is important to mention that the radiation beam of 15 MV provides a higher absorbed dose to all of the organs and tissues in each of the orientations.

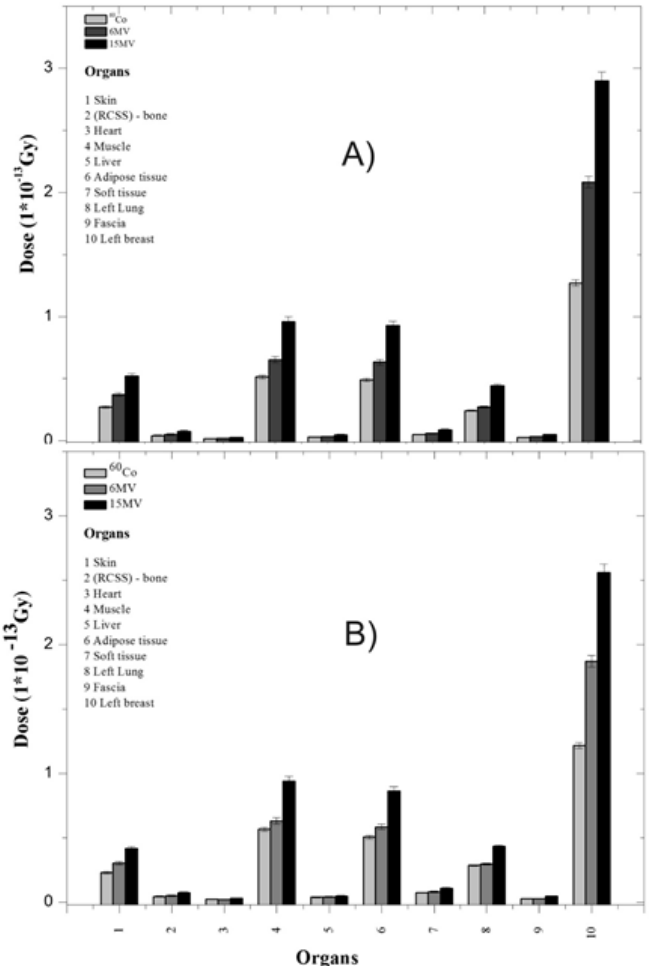

Figure 6 Dose absorbed in each of the orientations. A) Internal Tangential Field, B) External Tangential Field.

From the results of Tables 2 and 3 we could infer that the higher the energy, the greater the power of penetration and, therefore, in the skin and in the breast there would be smaller doses, however, if we observe the 15 MV spectrum of the Figure 4, a wide spectrum of photons below 1 MeV is found that generate a large contribution to the absorbed dose that is reflected in the results.

For the purposes of carrying out and independent analysis for each of the radiation beams, Tables 4, 5 and 6 show the results in dose percentage for each of the organs.

Various important aspects can be inferred from the data shown in Tables 4, 5 and 6. With respect to the absorbed dose of the target organ (the left breast), the internal tangential field with a beam of 6 MV transferred a 1.48% higher dose than the 15 MV beam, and 6.48% more than the dose provided by the ^{60}Co. The same analysis of the

external tangential field depicts that the 6 MV beam contributed an absorbed dose that is 1.42% greater than that of the 15 MV beam and 7.53% greater than the dose imparted from the ^{60}Co. This analysis shows that the 6 MV beam is more effective in the transfer of the dose to the target organ. Nevertheless, there are other considerations that must be made when analyzing the at-risk organs involved.

Table 2 Dose absorbed due to the two simulated fields

Organs	External Tangential			Internal Tangential		
	Co-60 (Gy)	6 MV	15 MV	Co-60 (Gy)	6 MV	15 MV
Skin	2.30E-14	3.02E-14	4.17E-14	2.73E-14	3.72E-14	5.21E-14
(RCSS) – Cortical bone	4.46E-15	5.04E-15	7.27E-15	4.10E-15	4.98E-15	7.50E-15
Muscle	5.68E-14	6.31E-14	9.38E-14	5.13E-14	6.53E-14	9.60E-14
Adipose tissue	5.06E-14	5.84E-14	8.64E-14	4.91-E14	6.34E-14	9.28E-14
Heart	2.32E-15	2.01E-15	2.90E-15	1.74E-15	1.86E-15	2.56E-15
Left lung	2.86E-14	2.97E-14	4.33E-14	2.43E-14	2.73E-14	4.45E-14
Left breast	1.22E-13	1.87E-13	2.56E-13	1.27E-13	2.08E-13	2.90E-13

Table 3 Sum of the contributions

Organs	Sum of contributions from the two fields		
	Co-60 (Gy)	6 MV	15 MV
Skin	5.03E-14	6.75E-14	9.39E-14
(RCSS) – Cortical bone	8.56E-15	1.00E-14	1.48E-14
Muscle	1.08E-13	1.28E-13	1.90E-13
Adipose tissue	9.97E-14	1.22E-13	1.79E-13
Heart	4.06E-15	3.87E-15	5.47E-15
Left lung	5.29E-14	5.70E-14	8.78E-14
Left breast	2.49E-13	3.95E-13	5.46E-13

Table 4 Percentage value of absorbed dose in each organ for the radiation beam of Co-60

Organs	External Tangential		Internal Tangential		Sum	
	Dose (Gy)	Dose %	Dose (Gy)	Dose %	Dose (Gy)	Dose %
Skin	2.30E-14	7.71	2.73E-14	9.33	5.03E-14	8.51
(RCSS) – Cortical bone	4.46E-15	1.49	4.10E-15	1.4	8.56E-15	1.45
Heart	2.32E-15	0.78	1.74E-15	0.59	4.06E-15	0.69
Muscle	5.68E-14	19	5.13E-14	17.51	1.08E-13	18.26
Liver	3.89E-15	1.3	2.85E-15	0.97	6.74E-15	1.14
Adipose Tissue	5.06E-14	16.94	4.91E-14	16.77	9.97E-14	16.86
Soft Tissue	7.39E15	2.47	5.08E-15	1.73	1.25E-14	2.11
Left Lung	2.86E-14	9.58	2.43E-14	8.3	5.29E-14	8.94
Left Breast	1.22E-13	40.73	1.27E-13	43.4	2.49E-13	42.05

Table 5 Percentage value of absorbed dose in each organ for the radiation beam of 6 MV

Organs	External Tangential		Internal Tangential		Sum	
	Dose (Gy)	Dose %	Dose (Gy)	Dose %	Dose (Gy)	Dose %
Skin	3.02E-14	7.80	3.72E-14	8.91	6.75E-14	8.38
(RCSS) – Cortical bone	5.04E-15	1.30	4.98E-15	1.19	1.00E-14	1.24
Heart	2.01E-15	0.52	1.86E-15	0.45	3.87E-15	0.48
Muscle	6.31E-14	16.28	6.53E-14	15.63	1.28E-13	15.94
Liver	4.13E-15	1.06	3.35E-15	0.80	7.48E-15	0.93
Adipose Tissue	5.84E-14	15.05	6.34E-14	15.17	1.22E-13	15.11
Soft Tissue	8.17E-15	2.11	6.01E-15	1.44	1.42E-14	1.76
Left Lung	2.97E-14	7.66	2.73E-14	6.53	5.70E-14	7.07
Left Breast	1.87E-13	48.23	2.08E-13	49.88	3.95E-13	49.08

Table 6 Percentage value of absorbed dose in each organ for the radiation beam of 15 MV

Another result that we consider to be important is that the contributions to the skin, muscle, and adipose tissue are much lower with the use of Co-60 when compared to the other photon beams that were used. This is an important aspect to bear in mind when considering that this beam of radiation would be appropriate for shallow treatments such as in the head and neck, or as seen in this case the breast.

The two most common energies in LINAC's today are 6 and 15 MV, if we analyze the results in organs at risk it is found that the higher the energy, the greater the LET and therefore the higher absorbed dose, the ideal would be to use 15 MV, however, and to counteract the production of photoneutrons that produce this energy, manufacturers have opted to use the 6 MV energy in the new techniques such as IMRT, IGRT and VMAT.

It is clear that the use of the photon beam on average with energy of 1.25 MeV has the characteristic of transferring its energy in the first cm, with penetration power lower than that obtained with the spectrum of 6 MV or with the spectrum of 15 MV. This aspect answers why the reduction in the dose.

Conclusion

Using Monte Carlo, the absorbed dose in organs and tissues was compared and evaluated during a breast cancer treatment using tangential fields and irradiating with three different energy beams.

The largest transfer of absorbed dose to the target organ corresponds to the 15 MV beam, nevertheless, the lowest absorbed dose in at-risk organs (heart and lungs) corresponds to beams of Co-60.

The differences in the absorbed dose provided to the target organ when using Co-60 and 6 MV are minimal. To the contrary, shallow organs such as skin, muscle, and adipose tissue receive lower doses when compared to the 6 and 15 MV beams. This aspect answers the question of why certain equipment such as the Gamma Knife are effective in treatments of the head even though they use sources of Co-60.

In conclusion, manufacturers should consider the possibility of manufacture equipment that use Co-60 with the qualities of a LINAC, that will have modern collimation systems (JAWS), and multi-leaf systems (MLC) that allow for the conformation of fields. This aspect is fundamental if the elevated costs of the maintenance of LINAC's is taken into account.

Acknowledgments

None.

Conflicts of interest

All authors declare no conflict of interest.

References

1. Lozano-Ascencio. R, Gómez-Dantés. H, Lewis. S, et al. Breast cancer trends in Latin America and the Caribbean. *Salud pública de México*. 2009;51:s147–s156.
2. Gomez-Iturriaga A, Moreno-Jimenez M, Martinez-Monge R. Radiotherapy treatment of breast cancer: standards and new trends. Accelerated partial breast irradiation. 2008;2(1).
3. Fourquet A, Campana F, Mosseri V, et al. Iridium-192 versus cobalt-60 boost in 3–7 cm breast cancer treated by irradiation alone: final results of a randomized trial. *Radiother Oncol*. 1995;34(2):114–120.
4. Kutcher GJ, Hunt M, McCormick B. Applicator for optimum cobalt-60 primary breast treatments. *Int J Radiat Oncol Biol Phys.* 1988;14(3):511–519.
5. Serizawa T, Iuchi T, Ono J, et al. Gamma knife treatment for multiple metastatic brain tumors compared with whole-brain radiation therapy. *J Neurosurg*. 2000;93:32–36.
6. Betti OO, Galmarini D, Derechinsky V, et al. Radiosurgery with a Linear Accelerator. Stereotactic and functional neurosurgery, 1991;57(1-2):87–98.
7. Adams EJ, Warrington AP. A comparison between cobalt and linear accelerator-based treatment plans for conformal and intensity-modulated radiotherapy. *Br J Radiol*. 2014;81(964):304–310.
8. Zhu C, Palmer GM, Breslin TM, et al. Diagnosis of breast cancer using fluorescence and diffuse reflectance spectroscopy: a Monte-Carlo-model-based approach. *J Biomed Opt.* 2008;13(3):034015.
9. Palmer GM, Zhu C, Breslin TM, et al. Monte Carlo-based inverse model for calculating tissue optical properties. Part II: Application to breast cancer diagnosis. *Appl Opt*. 2006;45(5):1072–1078.
10. Ma CM, Ding M, Li JS, et al. A comparative dosimetric study on tangential photon beams. intensity-modulated radiation therapy (IMRT) and modulated electron radiotherapy (MERT) for breast cancer treatment. *Phys Med Biol.* 2003;48(7):909.
11. Delis H, Spyrou G, Tzanakos G, et al. The influence of mammographic X-ray spectra on absorbed energy distribution in breast: Monte Carlo simulation studies. *Radiation measurements.* 2005;39(2):149-155.
12. Sheikh-Bagheri D, Rogers DWO. Monte Carlo calculation of nine megavoltage photon beam spectra using the BEAM code. *Med Phys.* 2002;29(3):391–402.
13. Neuenschwander H, Mackie TR, Reckwerdt PJ. MMC-a high-performance Monte Carlo code for electron beam treatment planning. *Phys Med Biol.* 1195;40(4):543.
14. Ding GX. Energy spectra, angular spread, fluence profiles and dose distributions of 6 and 18 MV photon beams: results of Monte Carlo simulations for a Varian 2100EX accelerator. *Phys Med Biol*. 2002;47(7):1025–1046.
15. Gómez-Ros JM, Bedogni R, Palermo I, et al. Design and validation of a photon insensitive multidetector neutron spectrometer based on Dysprosium activation foils. *Radiation Measurements.* 2011;46(12):1712–1715.
16. Taleei R, Shahriari M. Monte Carlo simulation of X-ray spectra and evaluation of filter effect using MCNP4C and FLUKA code. *Applied Radiation and Isotopes*. 2009;67(2):266-271.
17. Sempau J, Sanchez-Reyes A, Salvat F, et al. Monte Carlo simulation of electron beams from an accelerator head using PENELOPE. *Phys Med Biol.* 2001;46(4):1163–1186.
18. Kramer R, Khoury HJ, Vieira JW, et al. MAX06 and FAX06: update of two adult human phantoms for radiation protection dosimetry. *Phys Med Biol.* 2006;51(14):3331–3346.
19. Rasband WS. Image J software. National Institutes of Health: Bethesda, MD, USA, 2012.
20. MCNPX users manual version 2.5.0," edited by D. B. Pelowitz, Report No. LA-UR-02-2607 (Los Alamos National Laboratory, Los Alamos, 2005).
21. https://www.varian.com/oncology/products/software/treatment-planning/eclipse-treatment-planning-system
22. Jiménez JS, Lagos MD, Martinez-Ovalle SA. A Monte Carlo Study of the Photon Spectrum due to the Different Materials Used in the Construction of Flattening Filters of LINAC. Computational and mathematical methods in medicine, 2017.
23. Martínez-Ovalle S A, Barquero R. Gómez-Ros JM. et al. Neutron dosimetry in organs of an adult human phantom using linacs with multileaf collimator in radiotherapy treatments. Med Phys. 2012;39(5):2854–2866.